46th AIAA Aerospace Sciences Meeting and Exhibit
7 - 10 January 2008, Reno, Nevada

AIAA-2008-0281

46th AIAA Aerospace Sciences Meeting and Exhibit, January 7-10, 2008/Reno, Nevada

Extremum-Seeking Control of Subsonic Cavity Flow

Kihwan Kim*, Coşku Kasnakoğlu†, Andrea Serrani‡, and Mo Samimy§
The Ohio State University, Columbus, OH, USA

An adaptive control system using extremum-seeking optimization is developed to suppress subsonic cavity flow oscillations. The overall control system is developed by following two steps. First, a simple linear control law which uses measurements of wall pressure fluctuations at two different locations in the cavity is developed, and the effect on the magnitude of the limit cycle produced by tuning its control parameters, namely a gain K and a phase shift ϕ, is investigated analytically and experimentally. Then, an extremum-seeking algorithm is implemented to optimize the selection of the most critical control parameter, ϕ, in real time, in such a way that the magnitude of the limit cycle is minimized in closed-loop. A comparison with a linear-quadratic feedback controller based on a reduced-order model of the flow dynamics is presented and discussed. Experimental results highlight the advantage of parameter adaptation provided by the extremum-seeking algorithm over controllers of fixed structure when operating in off-design conditions.

I. Introduction

CLOSED-LOOP flow control is regarded as the most effective method to stabilize and improve the performance of fluid systems with minimized actuation efforts under various operating conditions.[1] In particular, cavity flow control has been the subject of intense investigation in the past ten years, due to its importance in aerodynamic applications. Flow over a shallow cavity produces self-sustained oscillations that result from the coupling between flow dynamics and flow-induced acoustic field.[2] These oscillations lead to strong resonant tones, which are known to cause, among other effects, structural damages on the mechanical systems that interact with the flow. Flow control applied to cavity flow systems aims at formulating strategies for suppressing or reducing the amplitude of the acoustic tones.[3,4] The flow control group at the Collaborative Center of Control Science at the Ohio State University in the past few years has developed and validated in experiments several approaches to feedback control for cavity flow oscillations in subsonic Mach numbers. An open-loop actuation scheme updated by a logic-based feedback law was originally proposed by Debiasi and Samimy.[5] Subsequently, a parallel-proportional with time-delay controller[6] and a neural-network approach[7] showed promising performances in attenuating cavity flow resonance. Recently, major advances have been achieved by employing a linear-quadratic controller designed on the basis of an experimentally-derived reduced-order flow model.[2]

In many applications, the goal of a feedback control system is to regulate certain output variables to optimize a given cost function. In this case, uncertainty in the cost function necessitates the use of adaptive algorithms to iteratively search for the optimal input such that the performance output is minimized. A control strategy that embeds a self-tuning mechanism to adaptively minimize a given cost function is termed *extremum-seeking control*.[8] Some advantages of extremum-seeking control over controllers of fixed structure can be summarized as follows:

*Post Doctoral Researcher, Dept. of Electrical & Computer Eng. and Dept. of Mechanical Eng., Member AIAA, kim.2189@osu.edu
†Graduate Student, Dept. of Electrical & Computer Eng., kasnakoglu.1@osu.edu
‡Assistant Professor, Dept. of Electrical & Computer Eng., Member AIAA, serrani.1@osu.edu
§Professor, Director of Gas Dynamics and Turbulence Laboratory, Dept. of Mechanical Eng., Associate Fellow AIAA, samimy.1@osu.edu

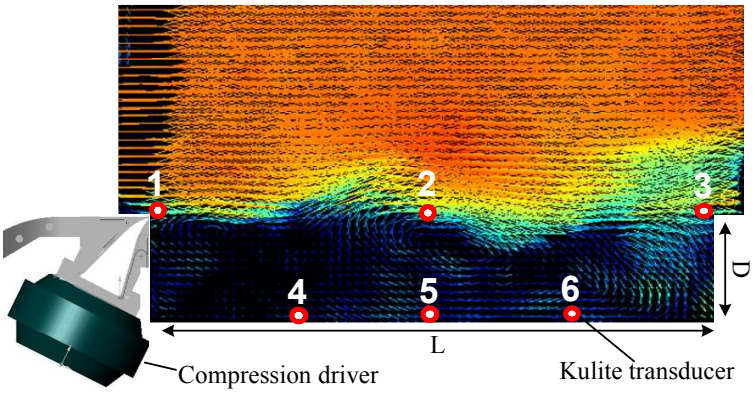

Figure 1. Schematic of the cavity with superimposed velocity vectors and magnitude obtained using PIV (baseline case at Mach 0.30 main flow). The locations of six pressure transducers are also shown.

- The application of extremum-seeking control does not require, in principle, a detailed control-oriented model of a plant. This is a particularly useful feature in case dynamic systems of interest are described by complex and/or uncertain models.
- It can be applied to a large class of nonlinear systems.
- It can be readily implemented in real-time applications, due to the relative simplicity of the tuning algorithm.

Extremum-seeking control has already been investigated in a variety of flow-related configurations, including backward-facing step,[9] bluff body,[10,11] diffuser,[12] and airfoil.[13] Applications to control of combustion instability and control of axial-flow compressors are reported respectively in Banaszuk et al.[14] and Wang et al.[15]

In this research, a control systems which includes an extremum-seeking algorithm is developed for suppressing subsonic cavity flow resonance. The magnitude of limit cycle, computed from two pressure fluctuation measurements, is employed as the performance output of the system. A simple but effective feedback control law characterized on the basis of a simplified Galerkin system proposed originally by Tadmor et al.[16] and Rowley and Juttijudata,[17] is employed as a baseline controller. The static input-output map of the closed-loop system between the controller parameters and the amplitude of the limit cycle in steady-state is derived analytically and identified experimentally. Then, an extremum-seeking feedback loop is applied on the closed-loop control system, thereby optimizing the parameters of the controller in real-time. As for the extremum-seeking scheme, the strategy implemented in this study follows the limit cycle minimization method presented in Wang and Krstić.[18] The extremum-seeking control is tested experimentally under different modes of cavity flow oscillation, e.g. single- and multi-resonance modes, so that its capability to adapt to different flow conditions can be investigated.

II. Experimental Setup

The experimental facility employed in this study is an optically accessible small scale blow-down wind tunnel located at the Gas Dynamics and Turbulence Laboratory of The Ohio State University. The tunnel can operate in the subsonic range between Mach 0.20 and Mach 0.70. Flow is directed to the 50.8 mm by 50.8 mm test section through a converging nozzle before exhausting to the atmosphere. As shown in Fig. 1, a shallow cavity is recessed in the test section with a depth D = 12.7 mm and length L = 50.8 mm for a length to depth aspect ratio L/D of four. The actuator consists of a Selenium D3300Ti compression driver connected to a 108 mm-long nozzle that converges from the driver to an exit slot of width 1 mm. The diaphragm movement of the compression driver creates oscillatory flow that exits through the slot at an angle of 30 deg with respect to the free-stream flow in the tunnel. The pressure fluctuations inside cavity are measured at 6 locations on the side wall by flush-mounted XCL-100-25A transducers. The signals pass through an anti-aliasing filter with a 10 kHz cutoff frequency. A dSpace 1103 DSP board operating at 50 kHz sampling rate is used to manage the data acquisition and the implementation of feedback control algorithms. Further details on the experimental setup and the actuator characteristics can be found in Refs. 5 and 19.

III. A Simple Feedback Controller for Cavity Flow Oscillation

In this section, a simple feedback law is derived for closed-loop control of cavity flow oscillation using a phasor model obtained from a simplified Galerkin system representing a reduced-order flow model. The type of controller employed in this study was originally proposed by Tadmor et al.[16] in the context of suppression of cylinder wake instability, and later considered by Rowley and Juttijudata[17] for cavity flows.

The considered reduced-order model of cavity flow, derived by means of Proper Orthogonal Decomposition and Galerkin projection techniques,[2,20] can be written in modal coordinates as[21]

$$\begin{aligned} \dot{\eta} &= F_1\eta + \varphi_1(\eta,\zeta) + (G_1 + \gamma_1(\eta,\zeta))\,u, \\ \dot{\zeta} &= F_2\zeta + \varphi_2(\eta,\zeta) + (G_2 + \gamma_2(\eta,\zeta))\,u, \end{aligned} \tag{1}$$

where $u \in \mathbb{R}$ stands for the control input,

$$\eta = \begin{pmatrix} \eta_1 \\ \eta_2 \end{pmatrix},\ \zeta = \begin{pmatrix} \zeta_1 \\ \vdots \\ \zeta_{N-2} \end{pmatrix},\ F_1 = \begin{bmatrix} \sigma & -\omega \\ \omega & \sigma \end{bmatrix},\ F_2 = \operatorname{diag}(-\lambda_1,\ldots,-\lambda_{N-2}),$$

$G_1 \in \mathbb{R}^2$, $G_2 \in \mathbb{R}^{N-2}$, $\varphi_1, \gamma_1 : \mathbb{R}^2 \times \mathbb{R}^{N-2} \to \mathbb{R}^2$, $\varphi_2, \gamma_2 : \mathbb{R}^2 \times \mathbb{R}^{N-2} \to \mathbb{R}^{N-2}$, and $\sigma > 0$, $\omega > 0$, $\lambda_i > 0$, $i = 1,\ldots,N$. In this Galerkin system, the state variable ζ accounts for a fast transient dynamics, while the state η describes the oscillatory behavior of the system. Elimination of ζ from Eq. (1) by means of a center-manifold reduction leads to a simple model of cavity flow oscillation as

$$\dot{\eta} = \begin{bmatrix} \sigma - \alpha\rho^2 & -\omega - \beta\rho^2 \\ \omega + \beta\rho^2 & \sigma - \alpha\rho^2 \end{bmatrix}\eta + \begin{bmatrix} b_1 \\ b_2 \end{bmatrix} u, \quad \text{where } \alpha > 0 \text{ and } \rho = \sqrt{\eta_1^2 + \eta_2^2}. \tag{2}$$

Using polar coordinates ρ and $\theta = \tan^{-1}(\eta_2/\eta_1)$, system Eq. (2) is transformed into the phasor model[16,17]

$$\dot{\rho} = \left(\sigma - \alpha\rho^2\right)\rho + (b_1\cos\theta + b_2\sin\theta)\,u, \tag{3a}$$

$$\dot{\theta} = \omega + \beta\rho^2 + \frac{1}{\rho}(b_2\cos\theta - b_1\sin\theta)\,u, \tag{3b}$$

where it is readily seen that, when $u = 0$, the magnitude ρ converges to a stable limit cycle with magnitude $\rho^* = \sqrt{\sigma/\alpha}$.

Compared with the original systems in Eq. (1), the model in Eq. (3) omits the detailed dynamics of cavity flow oscillation. However, it still preserves some of the key characteristics related to the limit cycle oscillation of the original model, and could be used to design a simple feedback controller.[17] To this end, consider the linear control law

$$u = -k_1\eta_1 - k_2\eta_2 = -K\rho\cos(\theta - \phi), \tag{4}$$

where $K = \sqrt{k_1^2 + k_2^2} > 0$ and $\phi = \tan^{-1}(k_2/k_1) \in [0,\ 2\pi]$. After application of this control law, averaging of Eq. (3a) with respect to $\theta \in [0, 2\pi]$ yields[17]

$$\dot{\rho} = \left(\sigma - \alpha\rho^2\right)\rho - K\rho\,(b_1\cos\phi + b_2\sin\phi). \tag{5}$$

The averaging theorem[22] allows an approximation of the solution of Eq. (5) with the solution of Eq. (3a). The effect of the control law in Eq. (4) on the magnitude of the limit cycle is to change ρ^* from $\sqrt{\sigma/\alpha}$ to

$$\rho^* = \sqrt{\frac{\sigma - K(b_1\cos\phi + b_2\sin\phi)}{\alpha}}, \tag{6}$$

where it is assumed that the magnitude of the control gains K is small enough to preserve the oscillation, that is, $K(b_1\cos\phi + b_2\sin\phi) < \sigma$. Note that the control u in Eq. (4) contains in principle two degrees of freedom, i.e., K and ϕ, which can both be used for the optimization of the control parameters. As noted in Refs. 16, 17, for each $K > 0$, tuning the phase ϕ to the optimal value ϕ_{opt} satisfying

$$\cos\phi_{\text{opt}} = b_1/|b|, \quad \sin\phi_{\text{opt}} = b_2/|b|,$$

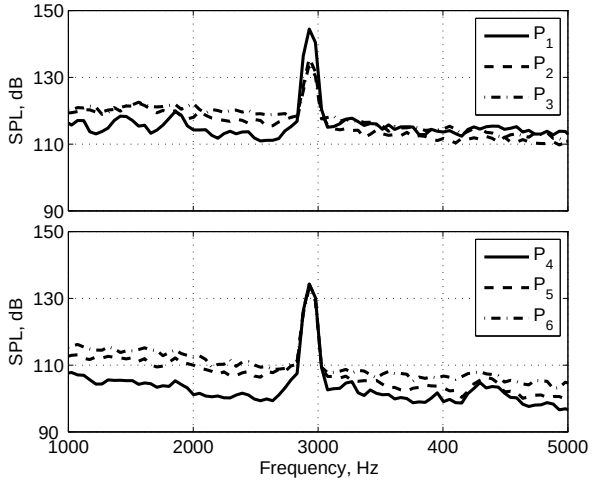

(a) SPL spectra of wall pressure fluctuation in the cavity.

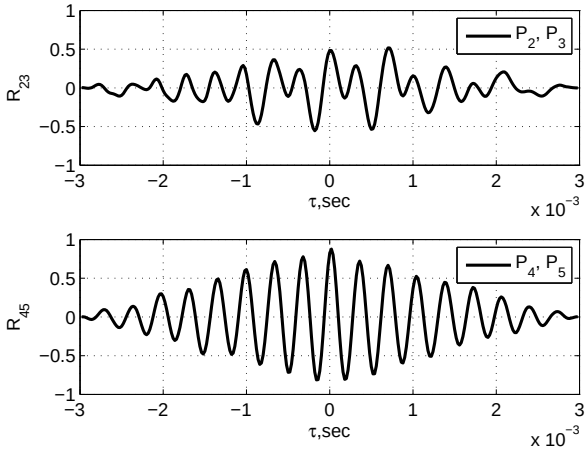

(b) Normalized cross-correlation for (P_2, P_3) and (P_4, P_5).

Figure 2. Characteristics of wall pressure fluctuations at Mach 0.30 baseline flow.

has the effect of minimizing ρ^* to the value

$$\rho^*_{\min} = \sqrt{\frac{\sigma - K\,|b|}{\alpha}}. \tag{7}$$

From Eq. (7), it is seen that increasing the gain K to $\sigma/|b|$ eventually forces the limit cycle oscillation to vanish, i.e. $\rho^*_{\min} \to 0$. This analytic result is in general different from what observed in experiments, where complete suppression of the oscillation can not be achieved by applying the control law in Eq (4). This is not surprising, since the analysis is based on a simplified reduced-order model which only captures the behavior of the system to a limited extent. Therefore, the characteristics of the proposed closed-loop control need to be verified from the cavity flow experiments, the results of which are compared to the analytical results in Eq. (6). Unfortunately, it is not viable to implement this control scheme directly to a cavity flow configuration, since the state variables η cannot be measured in real time from the flow field. However, assuming a linear relation $p = C\eta,\ C \in \mathbb{R}^{2\times 2}$ between η and a pair of local pressure measurements $p = (p_a,\, p_b)^T$ facilitates reformulating Eq. (4) as:

$$u = -K\rho\cos\left(\theta - \phi\right) = -\begin{bmatrix} k_1 & k_2 \end{bmatrix} C^{-1} p = -\tilde{K}\tilde{\rho}\cos\left(\tilde{\theta} - \tilde{\phi}\right), \tag{8}$$

where $\tilde{\rho} = \sqrt{p_a^2 + p_b^2}$, $\tilde{\theta} = \arctan\left(p_b/p_a\right)$. Note that the control law in Eq. (8) has exactly the same structure as the original controller in Eq. (4). As a result, the same control strategy can be implemented in terms of feedback from independent pressure measurements instead of state variables. Obviously, for any given flow configuration, the actual computation of the parameters $(\tilde{K}, \tilde{\phi})$ requires knowledge of the plant model parameters, including the output map C, which are affected by a large uncertainty due to the approximate nature of the phasor model (3). However, this limitation will be overcome by the self-tuning mechanism embedded in the extremum-seeking controller. For notational convenience, the notation $\tilde{(\cdot)}$ will be omitted for the remainder of the paper, with the understanding that the controller parameters refer to Eq. (8).

Basically, the state variables η_1 and η_2 in Eq. (4) represent the system dynamics associated with the limit cycle oscillation. Therefore, the two signals p_a and p_b employed for feedback should possess the same dynamical characteristics as η. The rationale behind the selection of two best signals among several available pressure measurements is based on the following criteria:

- The two pressure signals should be strongly correlated. The cross-correlation indicating the similarity between two signals can be estimated and normalized based on N samples of the signals u and v as

$$R_{uv}(m) = \frac{1}{R_{uu}(0)R_{vv}(0)} \cdot \begin{cases} \sum\limits_{n=0}^{N-m-1} u\left[n+m\right] v\left[n\right], & m \geqslant 0 \\ R_{vu}(-m), & m < 0 \end{cases} \tag{9}$$

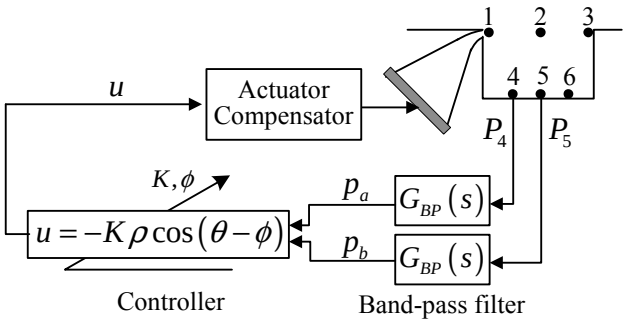

Figure 3. Inner-loop control system.

where $-N + 1 \leq m \leq N - 1$.

- The signal-to-noise (S/N) ratio of the selected signal should be the largest possible. The S/N ratio carried by each pressure signal can be examined graphically from the sound-pressure-level (SPL) spectra, by comparing the magnitude of the resonance peak with the background noise level.

Figure 2(a) shows the SPL spectra of all wall pressure fluctuations measured at six locations as shown in Figure 1 in Mach 0.30 baseline flow. The signals $P_i, i = 1 \ldots 6$ stand for the pressure fluctuations at each location shown in Fig. 3. While the SPL of all pressure signals exhibits a strong resonance peak at about 2.9 kHz, the background noise levels of P_1, P_2, and P_3 located at the shear layer are considerably higher than those of sensors P_4, P_5, and P_6, located at the bottom of the cavity. The number of all possible pairs from the 6 pressure measurements is 15. As shown in Fig. 2(b), the cross-correlation analysis in Eq. (9) for all 15 pairs results in the pair (P_2, P_3) having the weakest cross-correlation and the pair (P_4, P_5) exhibiting the strongest cross-correlation. As a result, the pair (P_4, P_5) is selected as the output for the feedback controller given in Eq. (8). To further reduce the background noise level, the signals P_4 and P_5 are then filtered by a pair of 4th-order Butterworth bandpass filters, $G_{BP}(s)$, having a passband of 1.5 kHz - 4 kHz. In addition, the actuator compensator derived in Ref.[19] is embedded in the control loop. The synthetic jet-like actuator employed in the experimental setup possesses a strong dynamic characteristic, which severely distorts the control signal. A servo-compensator designed using H_∞ control theory forces the actuator output to track the control signal u such that the uncertainty caused by the actuator dynamics can be effectively compensated, and its effect ignored in closed-loop. Figure 3 shows the experimental implementation of the proposed control law.

Next, the static map between ρ^* and $(K,\ \phi)$ is identified in closed-loop experiments on the baseline Mach 0.30 flow. The control parameters $(K,\ \phi)$ are manually tuned, and the corresponding averaged amplitude

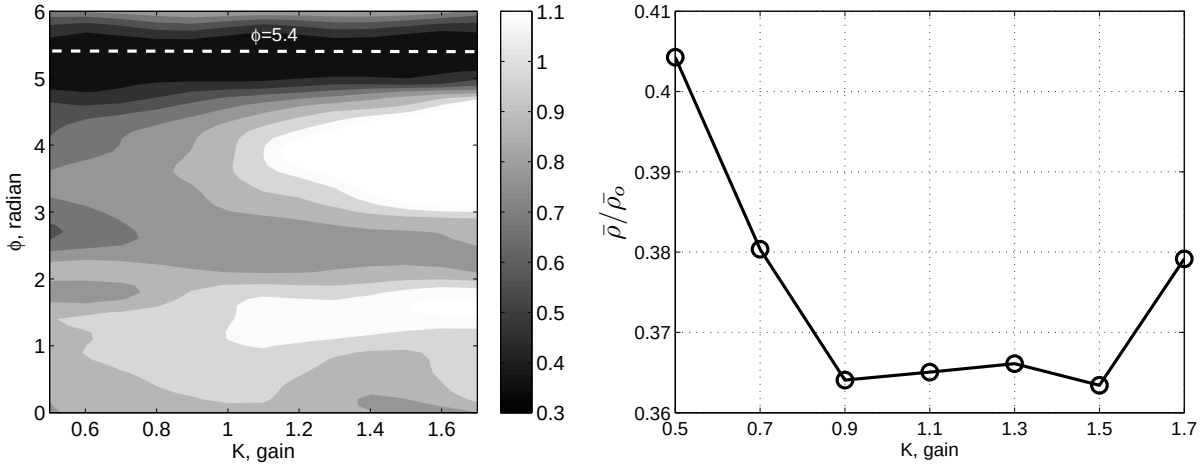

(a) Averaged limit cycle magnitude, $\bar{\rho}$.

(b) Effect of K on $\bar{\rho}$ ($\phi = 5.4$).

Figure 4. Averaged limit cycle magnitude, $\bar{\rho}/\bar{\rho}_o$, with respect to control parameters K and ϕ. $\bar{\rho}_o = 0.36$ kPa.

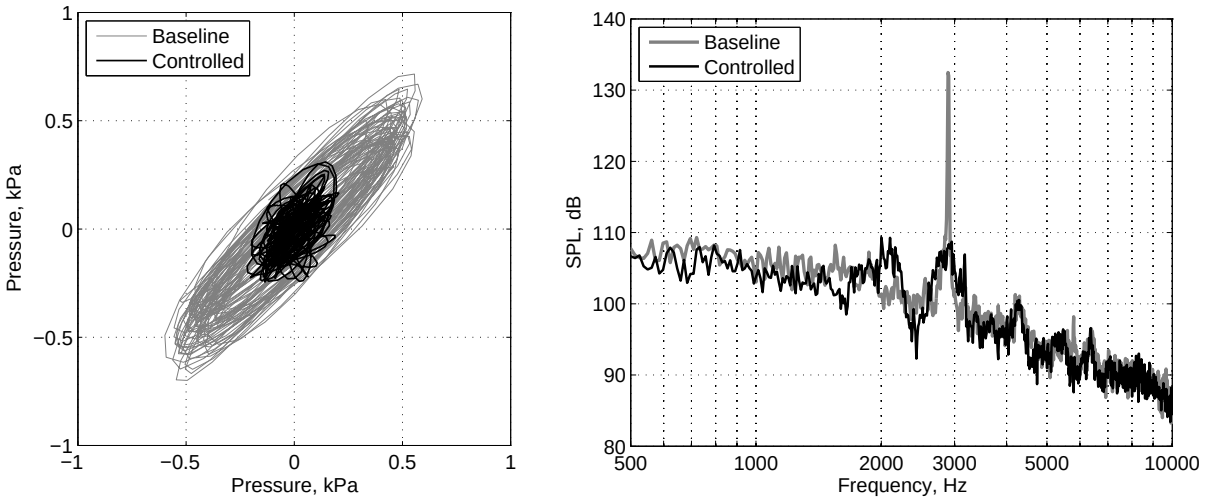

(a) Phase plot. x-axis:p_a and y-axis:p_b.

(b) SPL spectra at the transducer 5.

Figure 5. Performance of the closed-loop control at Mach 0.30 flow. The control parameters are set as $K = 1.0, \phi = 5.4$.

of the oscillation in steady-state, $\bar{\rho}$, is computed. A plot of $\bar{\rho}$ versus the controller parameters (K, ϕ) is shown in Fig 4, where the magnitude $\bar{\rho}$ is normalized by the averaged limit cycle magnitude of the baseline flow, $\bar{\rho}_o = 0.36$ kPa. It is seen from Fig. 4(a) that the experimental results are in good agreement with the analysis in Eq. (6) as far as the variation of the phase shift parameter ϕ is concerned. There exists an optimal value $\phi_{opt} = 5.4$ rad for this controller parameter where $\bar{\rho}$ is minimized, irrespective of the value of K in the given range. However, the effect of variations of K does not match the analytical model. At $\phi = 5.4$, as K increases, the magnitude ρ tends to decrease initially but then increases again when $K > 1.5$. Conversely, Eq. (7) predicts a monotonic attenuation of the limit cycle magnitude with increasing K when ϕ is set to the optimal value ϕ_{opt}. This result implies that the simple averaged model in Eq. (5) leads to a considerable difference between the real effect of K on ρ^*_{min} and the analytical relationship in Eq. (7).

Finally, Figure 5 shows the performance of the control system corresponding to $K = 1.0, \phi = 5.4$, which is hereby regarded as the optimal parameter set. The phase plot in Fig. 5(a) shows that the limit cycle magnitude in closed-loop is considerably decreased compared to the baseline case. This is confirmed by Fig. 5(b), where it is shown that the resonance peak in the SPL spectrum is reduced by 22 dB in closed-loop.

IV. Extremum-Seeking Optimization of Control Parameters

The next step is the formulation of an extremum-seeking algorithm to adaptively tune the controller parameters on-line. As mentioned earlier, the extremum-seeking scheme has in principle two degrees of freedom for the optimization, corresponding to the parameters K and ϕ. However, adapting K will not be appropriate for controller considered here, for the following reasons:

- Increasing K may cause actuator saturation, and thus its effect will be limited.
- The sensitivity of ρ^* with K is much smaller than that of ϕ.
- The phase shift ϕ determines the sign of the feedback action, and thus its effect is crucial in determining attenuation or amplification of the limit cycle.

These characteristics can be clearly observed in Fig. 4. Consequently, the gain K is kept constant at $K = 1.0$ and only the phase ϕ is adapted in this research.

The structure of the single parameter extremum-seeking optimization algorithm, inspired by Wang and Kristić,[18] is shown in Figure 6. The extremum-seeking controller acts as an outer-loop to the controller in Figure 3. The scheme implements a gradient-based online optimization using an estimate of the sensitivity of ρ^* with respect to ϕ obtained using a sinusoidal perturbation $\Delta\phi$. The control parameter ϕ can be adapted in

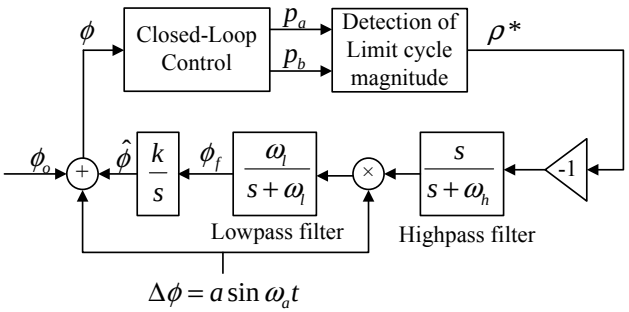

Figure 6. Outer feedback loop using extremum-seeking algorithm.

real time using a gradient descent method to achieve the minimum of the limit cycle magnitude, ρ^*. A simple detection algorithm of limit cycle magnitude can be established as follows: Assuming that $p_a = r_a \cos\omega t$ and $p_b = r_b \sin\omega t$, the squared magnitude ρ^2 becomes

$$\rho^2 = p_a^2 + p_b^2 = \frac{\left(r_a^2 + r_b^2\right)}{2} + \frac{\left(r_a^2 - r_b^2\right)}{2}\cos 2\omega t. \tag{10}$$

The squared signal ρ^2 is filtered through a low-pass filter $G_L(s)$. Provided that the bandwidth ω_L of $G_L(s)$ satisfies the condition $\omega_L \ll \omega$, the filter $G_L(s)$ allows the extraction of the time-invariant component from Eq. (10) as

$$\rho^* = \sqrt{\tfrac{1}{2}\left(r_a^2 + r_b^2\right)}.$$

Suppose that the static input-output map $f : \phi \to \rho^*$ representing the relationship between ϕ and ρ^* has a minimum. In the vicinity of an initial value $\phi = \phi_o$, the map f can be approximated by Taylor series as

$$\rho^* = f(\phi) \approx f(\phi_o) + f'(\phi_o)\Delta\phi = f(\phi_o) + f'(\phi_o)a\sin(\omega_a t), \tag{11}$$

where $\Delta\phi = a\sin(\omega_a t), a \ll O(\phi)$ is a perturbation signal. In the scheme in Fig. 6, the perturbation is implemented as an additive sinusoidal signal, whose frequency ω_a is sufficiently small such that the static relationship $\rho^* = f(\phi)$ is maintained. From Fig. 6, the bandwidth ω_h and ω_l of high-pass and low-pass filters, respectively, are chosen to satisfy the condition $\omega_h,\ \omega_l \ll \omega_a$. As a result, the output ϕ_f of a low-pass filter $\omega_l/(s+\omega_l)$ becomes

$$\phi_f \approx -f'(\phi_o)\frac{a^2}{2}, \tag{12}$$

which facilitates the detection of the gradient $f'(\phi_o)$ without the exact knowledge of the map. The relationship between the filter output ϕ_f and the update $\hat{\phi}$ is chosen as

$$\dot{\hat{\phi}} = k \cdot \phi_f.$$

The value of $\hat{\phi}$ is updated by the integration of ϕ_f every time step, until ρ^* approaches the minimum where $f'(\phi) = 0$. For the sake of stable and effective extremum-seeking optimization, the following relationships should be established:[8]

$$\begin{aligned}&\text{Cavity oscillation frequency, } \omega > \text{Cutoff frequency for limit cycle detection, } \omega_L > \\ &\text{Perturbation, } \omega_a > \text{Filter frequencies, } \omega_l,\ \omega_h.\end{aligned} \tag{13}$$

In what follows, the selection of the parameters of the filters in the extremum-seeking loop are discussed based on the conditions given in Eq. (13). First of all, a third-order Butterworth low-pass filter with a cutoff frequency $\omega_L/2\pi$ =50 Hz is chosen for the filter G_L used to compute the limit cycle magnitude. Note that the designed cutoff frequency at 50 Hz is considerably lower than the frequency range of interest in cavity flow oscillation, namely 2-4 kHz. To determine the perturbation frequency ω_a, ϕ is varied from 0 to 2π at a given frequency f_a as follows

$$\phi = \pi + \pi\sin(\omega_a t), \text{with } \omega_a = 2\pi f_a, \tag{14}$$

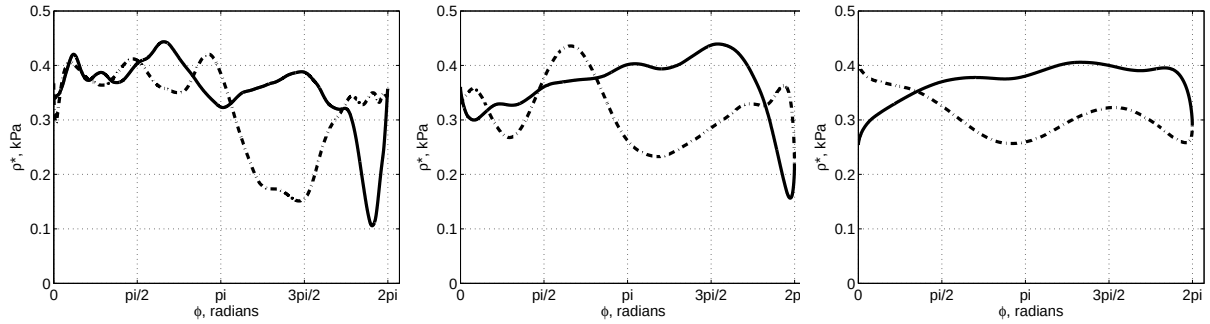

(a) $f_a = 4$ Hz (b) $f_a = 8$ Hz (c) $f_a = 16$ Hz

Figure 7. Effects of perturbation frequency f_a on the relationship between ρ^* and ϕ.

and the effect of each f_a on the relationship between ρ^* and ϕ is analyzed. Note that the extremum-seeking loop is not active during this investigation. The result of the analysis is shown in Fig. 7, where the solid lines account for increasing values of ϕ from 0 to 2π, while the dashed lines account for decreasing values from 2π to 0. At $f_a = 4$ Hz, the relationship between ϕ and ρ^* is very similar to the characteristic of the averaged limit cycle magnitude shown in Fig. 4(a), as it possesses a minimum around 1.5π-2π, although the minimum value is shifted slightly depending on the direction of varying ϕ. As the frequency f_a increases to 8 Hz and 16 Hz, the relationship loses the key characteristic of the existence of a minimum value. Consequently, the perturbation signal is set as $\Delta\phi = 0.1\sin(2\pi \cdot 3 \cdot t)$, where the frequency is lower than 4 Hz and the amplitude is smaller than the order $O(\phi) \approx 1$. Subsequently, both filter frequencies ω_h and ω_l are set at 0.4 Hz. to satisfy the condition in Eq. (13).

The resulting extremum-seeking controller is tested in closed-loop experiments at the baseline Mach 0.3 flow, with an initial value $\phi_o = 4.5$. As shown in Fig. 8, the parameter ϕ is updated successfully from 4.5 to 5.39 until the limit cycle magnitude ρ^* reaches its minimum value about 0.15 kPa. Figure 9 verifies the effectiveness of the extremum-seeking control on the SPL spectrogram recorded using pressure transducer #5. The resonance peak at around 2.9 Hz is gradually attenuated, following the reduction of the magnitude ρ^*.

V. Comparison to Fixed-Structure Flow Control

In this section, the performance of the extremum-seeking controller is compared with that of the linear quadratic (LQ) controller developed in Samimy et al.,[2] whose scheme is shown in Fig. 10. The LQ controller is developed on the basis of a 4th-order reduced-order flow model, obtained at Mach 0.30 baseline flow by

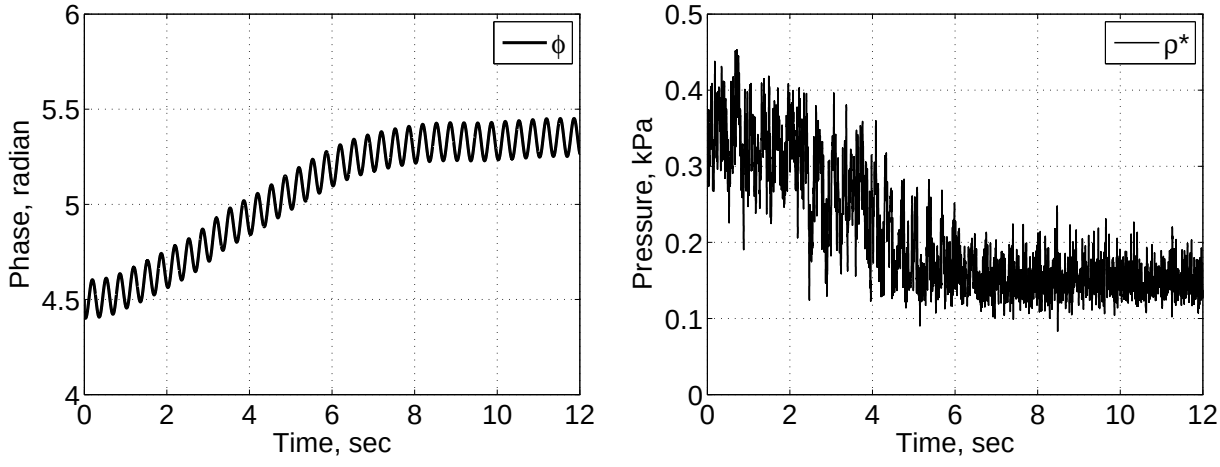

(a) Control parameter ϕ (b) Limit cycle magnitude ρ^*

Figure 8. Transient characteristics of the extremum-seeking control. The initial value of ϕ is 4.5.

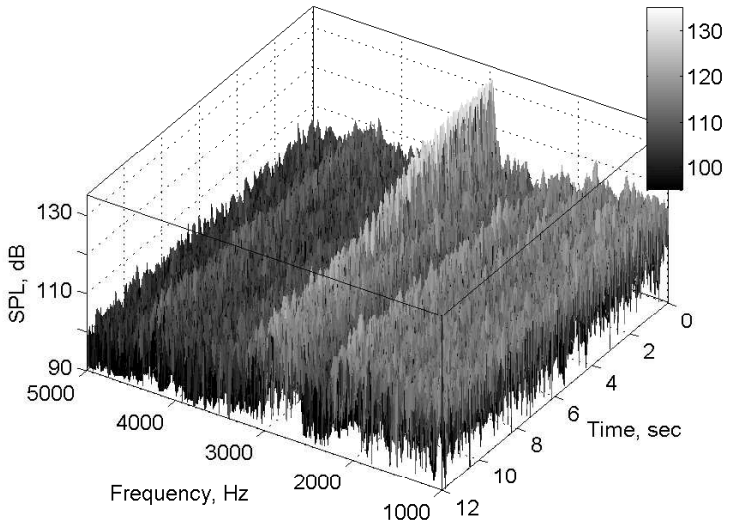

Figure 9. SPL spectrogram measured at the transducer 5 in transition under ES control.

means of proper orthogonal decomposition (POD) and Galerkin projection methods. The resulting linearized flow model is written as

$$\dot{\mathbf{a}}(t) = G\mathbf{a}(t) + Bu(t), \tag{15}$$

where the vector $\mathbf{a} \in \mathbb{R}^{4\times 1}$ stands for the modal coefficients of the POD expansion. Quadratic stochastic estimation is implemented to correlate real-time measurements of surface pressure fluctuations $P_j(t)$ at m distinct locations with $\mathbf{a}$ in Eq. (15). The estimated states $\hat{a}_i \in \hat{\mathbf{a}}$ are defined as

$$\hat{a}_i(t) = C^{ij}P_j(t) + D^{ijk}P_j(t)P_k(t), \quad i = 1\ldots 4, \quad j,k = 1\ldots m. \tag{16}$$

In this study, surface pressure measurements were obtained at the four distinct locations labeled $2, 4, 5, 6$ in Fig. 10. The structure of the LQ controller is given by

$$u(t) = -K_{LQ}\hat{\mathbf{a}}(t), \tag{17}$$

where the gain matrix $K_{LQ} \in \mathbb{R}^{1\times 4}$ minimizes a quadratic cost function of the system states and the input energy.[23] The major difference between the extremum-seeking controller and the LQ control is the adaptability of the control parameters. The gain matrix K_{LQ} of the LQ controller is determined on the basis of the model identified at a given design condition (e.g. Mach 0.30 flow in this study), and is therefore fixed irrespective of the actual flow condition. In contrast, the parameter ϕ of the extremum-seeking control is determined in real time, which in principle yields a means to account for varying flow conditions.

Figure 11(a) shows a comparison between the LQ controller and the extremum-seeking controller in closed-loop experiments using SPL spectra measured at transducer #5. In this example, the freestream

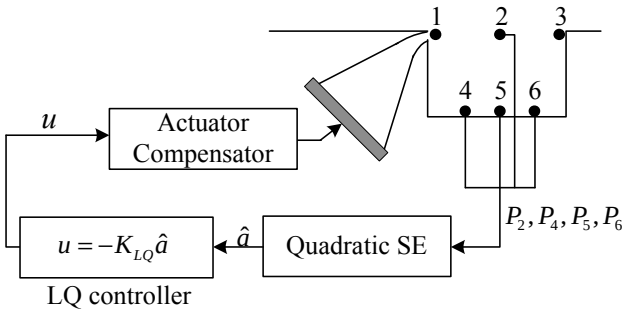

Figure 10. Linear quadratic feedback system for cavity flows. Pressure transducers 2, 4, 5, and 6 are used for stochastic estimation of system variables.

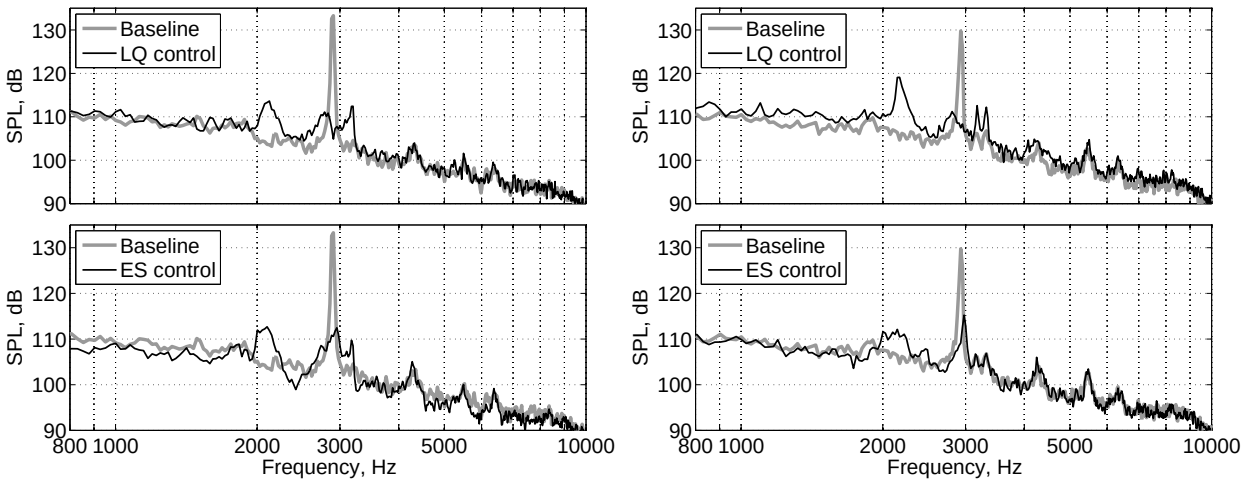

(a) Mach 0.30 (b) Mach 0.32

Figure 11. SPL spectra measured at the transducer 5 under LQ control (top) and extremum-seeking control (bottom) at Mach 0.30 and 0.32 flows, respectively.

Mach number is set to design condition (Mach 0.3) for the LQ control system. Both control systems show a successful and similar performance: The resonance peaks are reduced by about 20 dB, and the overall SPL level is suppressed to approximately below 110 dB. In the extremum-seeking control, the averaged value of the parameter ϕ converges to $\phi = 5.39$, which is almost identical to 5.4, the optimal value identified during the closed-loop experiments in Section III. Therefore, the extremum-seeking control is verified to operate correctly. Figure 11(b) shows the effectiveness of the control systems when the Mach number is increased to 0.32. The performance of the LQ control starts deteriorating as the flow condition deviates from the design condition. The resonance peak is still suppressed, whereas the peak at around 2.2 kHz is considerably amplified. In contrast, the extremum-seeking control maintains a level of performance similar to the results at Mach 0.30. In this case , the parameter ϕ is changed from 5.39 to 2.58. As shown in Fig. 12, as the Mach number increases further beyond 0.32, the characteristics of the cavity flow oscillation changes from a single-resonance mode to a multi-resonance mode, where a first peak is generated at 2.4 kHz and a second peak at 3.4 kHz. At this flow condition, the LQ control amplifies significantly the peak at 2.2 kHz, even though it attenuates the second peak of the baseline flow. In addition, the noise level below 2 kHz is increased. On

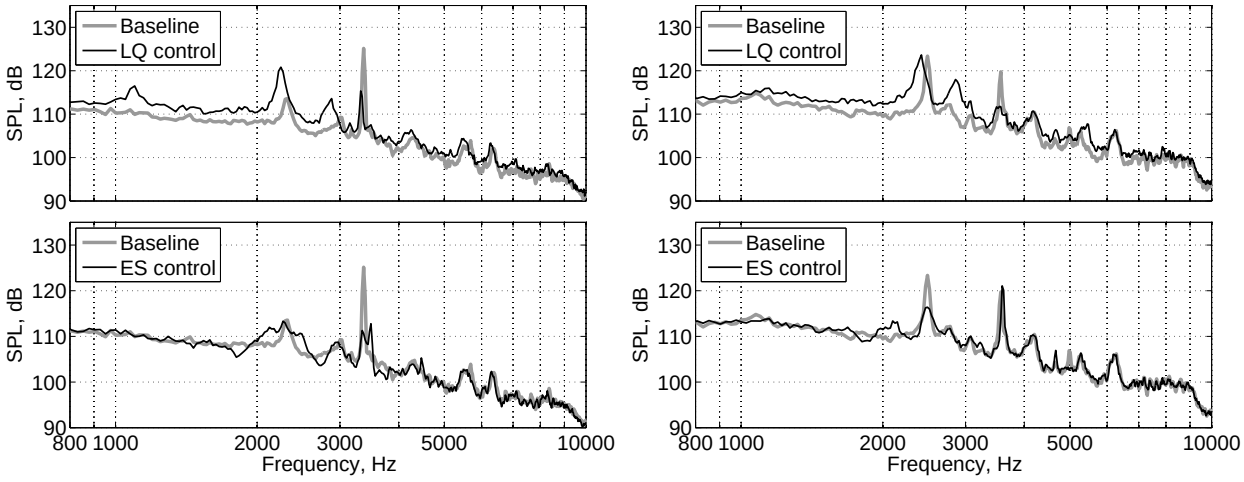

(a) Mach 0.34 (b) Mach 0.38

Figure 12. SPL spectra measured at the transducer 5 under LQ control (top) and extremum-seeking control (bottom) at Mach 0.34 and 0.38 flows, respectively.

Mach number	0.28	0.30	0.32	0.34	0.38
ϕ	5.43	5.39	2.58	2.33	2.45

Table 1. Adaptation of the parameter ϕ with respect to Mach numbers.

the other end, the extremum-seeking control is still effective, as shown in Fig. 12(a). At Mach 0.38 (strong multi-resonance mode) shown in Fig. 12(b), the extremum-seeking control succeeds in suppressing the first peak of the baseline flow, but barely affects the second peak. However, it does not generates any side effects, differently from the LQ control. It is worth noting that the extremum-seeking controller suppresses the tone with the highest SPL, which in this case is the one at 2.4 kHz, which is consistent with the fact that the algorithm does not possess any information on the frequency of the limit cycle. This also suggests that the current single-parameter adaptive scheme is not sufficient for handling a multi-resonance mode, and a multi-parameter scheme would be required instead. Table 1 lists the variation of ϕ with respect to different Mach numbers.

As a final performance indicator, the variation of the overall sound pressure level (OASPL) is computed as the difference between the OASPLs of controlled and baseline cases

$$\Delta OASPL = OASPL_{controlled} - OASPL_{baseline},$$

with

$$OASPL = 20\log_{10}\left[\frac{1}{m}\sum_{i=1}^{m}\left\{\frac{1}{P_o}\sqrt{\frac{1}{n}\sum_{j=1}^{n}|P_i(j)|^2}\right\}\right] \quad \text{(dB)},$$

where the reference pressure $P_o = 20$ μPa. The SPL data computed from each transducer($m = 6$) are averaged to obtain the OASPL. As shown in fig. 13, the trend in $\Delta OASPL$ with respect to Mach numbers shows the clear advantage of extremum-seeking control over fixed-structure control systems. While the LQ control brings the benefits only in the design condition (Mach 0.30) and its neighborhood (Mach 0.28 and 0.32), the extremum-seeking control shows better performance at single-resonance modes than the LQ control and maintains its effectiveness to some degree even at multi-resonance modes.

VI. Conclusions

Varying flow condition in a subsonic shallow cavity flow affects the dynamic characteristics of cavity flow resonance. In our configuration, increasing the Mach number from 0.30 to 0.38 changes the resonance significantly from single mode to multiple modes. This research developed the adaptive flow control system using extremum-seeking algorithm, which aims at adapting the control parameters to maximize the attenuation of the flow resonance at flow conditions.

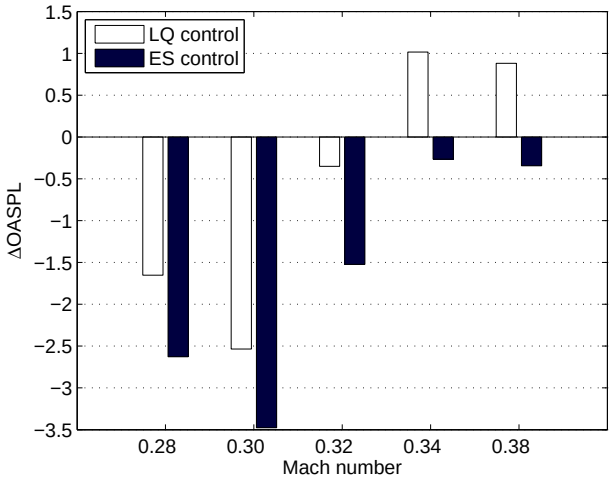

Figure 13. Comparison of Extremum-seeking control and LQ control in terms of change of overall SPL ($\Delta OASPL$) for different Mach numbers.

First, an inner closed-loop control system was developed using a simple, pressure-based control law. The effects of the control parameters, i.e. gain K and phase ϕ, on the limit cycle magnitude ρ were identified analytically and experimentally. It was verified from both analytical relationships and experimental results that there exists an optimal value ϕ_{OPT} of the controller parameter where ρ is minimized, regardless of K. As for the effects of K, the analytical results are not matched with the experimental results. It is due to the simplicity of a phasor model derived from a Galerkin system. Therefore, extremum-seeking optimization was applied only to the parameter ϕ, with K fixed at 1.0. As for the extremum-seeking scheme, the gradient-based searching algorithm with a sinusoidal perturbation was implemented. The effectiveness of the extremum-seeking control was verified under various flow Mach numbers. The experimental results were compared with those obtained with a linear-quadratic feedback control based on a reduced-order Galerkin model representing a class of fixed-structure control systems. While the LQ control attenuates the resonance only at Mach numbers close to the design condition, the extremum-seeking control extends the range of Mach numbers where the control is effective by tuning the control parameter automatically.

Acknowledgments

This work is supported in part by the AFRL/VA and AFOSR through the Collaborative Center of Control Science (Contract F33615-01-2-3154). The authors would like to thank their colleagues at CCCS, James Myatt, Chris Camphouse, Edgar Caraballo and Jesse Little for assistance and fruitful discussions.

References

[1]Ga-del-Hak, M., *Flow Control: Passive, Active, and Reactive Flow Management*, Cambridge Univ. Press, 2004.

[2]Samimy, M., Debiasi, M., Caraballo, E., Serrani, A., Yuan, X., Little, J., and Myatt, J. H., "Feedback Control of Subsonic Cavity Flows Using Reduced-Order Models," *Journal of Fluid Mechanics*, Vol. 579, 2007, pp. 315–346.

[3]Rowley, C. and Williams, D. R., "Dynamics and Control of High-Reynolds-Number Flow over Open Cavities," *Annual Review of Fluid Mechnics*, Vol. 38, 2006, pp. 251–276.

[4]Cattafesta, L. N., Williams, D. R., Rowley, C. W., and Alvi, F. S., "Review of Active Control of Flow-Induced Cavity Resonance," AIAA Paper 2003-3567, 2003.

[5]Debiasi, M. and Samimy, M., "Logic-Based Active Control of Subsonic Cavity Flow Resonance," *AIAA Journal*, Vol. 42, No. 9, Sep 2004, pp. 1901–1909.

[6]Yan, P., Debiasi, M., Yuan, X., Little, J., Özbay, H., and Samimy, M., "Experimental Study of Linear Closed-Loop Control of Subsonic Cavity Flow," *AIAA Journal*, Vol. 44, No. 5, 2006, pp. 929–938.

[7]Efe, M. Ö., Debiasi, M., Yan, P., Özbay, H., and Samimy, M., "Control of Subsonic Cavity Flows by Neural Networks - Analytical Models and Experimental Validation," AIAA Paper 2005-0294, 2005.

[8]Ariyur, K. B. and Krstić, M., *Real-Time Optimization by Extremum-Seeking Control*, John Wiley & Sons, Hoboken, NJ, 2003.

[9]Garwon, M. and King, R., "A Multivariable Adaptive Control Strategy to Regulate the Separated Flow Behind a Backward-Facing Step," *Proceedings of the 16th IFAC World Congress*, Prague, Czech Republic, 2005.

[10]Henning, L. and King, R., "Drag Reduction by Closed-Loop Control of a Separated Flow over a Bluff Body with a Blunt Trailing Edge." *Proceedings of the 44th IEEE Conference on Decision and Control and European Control Confernce*, Seville, Spain, 2005, pp. 494–499.

[11]Beaudoin, J.-F., Cadot, O., Aider, J.-L., and Wesfried, J.-E., "Drag Reduction of a Bluff Body Using Adaptive Control Methods," *Physics of Fluids*, Vol. 18, No. 8, 2006, pp. 085107–1– 085107–10.

[12]Banaszuk, A. and Narayanan, S., "Adaptive Control of Flow Separation in a Planar Diffuser," AIAA Paper 2003-0617, 2003.

[13]Becker, R., King, R., Petz, R., and Nitsche, W., "Adaptive Closed-Loop Separation control on a High-Lift Configuration Using Extremum Seeking," *AIAA Journal*, Vol. 45, No. 6, 2007, pp. 1382–1392.

[14]Banaszuk, A., Ariyur, K. B., M.Krstić, and Jacobson, C. A., "An adaptive algorithm for control of combustion instability," *Automatica*, Vol. 40, No. 11, 2004, pp. 1965–1972.

[15]Wang, H.-H., Yeung, S., and Krstić, M., "Experimental application of extremum seeking on an axial-flow compressor," *IEEE Transactions on Control Systems Technology*, Vol. 8, No. 2, 2000, pp. 300–309.

[16]Tadmor, G., Noack, B. R., Morzyński, M., and Siegel, S., "Low-Dimensional Models for Feedback Flow Control. Part II: Control Design and Dynamic Estimation," AIAA Paper 2004-2409, 2004.

[17]Rowley, C. W. and Juttijudata, V., "Model-Based Control and Estimation of Cavity Flow Oscillations," *Proceedings of the 44th IEEE Conference on Decision and Control*, 2005, pp. 512–517.

[18]Wang, H.-H. and Krstić, M., "Extremum Seeking for Limit Cycle Minimization," *IEEE Transactions on Automatic Control*, Vol. 45, No. 12, 2000, pp. 2432–2437.

[19]Kim, K., Debiasi, M., Schultz, R., Serrani, A., and Samimy, M., "Dynamic Compensation of a Synthetic Jet-Like Actuator for Closed-Loop Cavity Flow Control," Accepted for publication on *AIAA Journal*, 2007.

[20]Rowley, C. W., Colonius, T., and Murray, R. M., "Model Reduction for Compressible Flows Using POD and Galerkin Projection," *Physica D*, Vol. 189, No. 1-2, 2004, pp. 115–29.

[21]Kasnakoğlu, C. and Serrani, A., "Oscillation Supression in Galerkin Systems Using Center-Manifold and Averaging Techniques," *European Journal of Control*, Vol. 5, 2007, pp. 1–14.

[22]Guckenheimer, J. and Holmes, P., *Nonlinear Oscillations, Dynamical Systems, and Bifurcations of Vector Fields*, Vol. 42 of *Applied Mathematical Sciences*, Springer, 3rd ed., 1983.

[23]Skogestad, S. and Postlethwaite, I., *Multivariable Feedback Control*, Wiley, West Sussex, England, 2nd ed., 2005.